

Quantum Statistical Parton Distributions and the Spin Crisis

F. Buccella, G. Miele and N. Tancredi

Dipartimento di Scienze Fisiche, Università di Napoli "Federico II", and INFN Sezione di Napoli, Mostra D'Oltremare Pad. 20, I-80125 Napoli, Italy

Abstract

Quantum statistical distributions for the partons provide a fair description of deep inelastic scattering data at $Q^2 = 3$ and 10 (GeV/c)^2 . The study of the polarized structure functions seems to suggest an alternative possible solution of the *spin crisis* based on the Pauli principle. In this scheme, in fact, the defects of the Gottfried sum rule and Ellis–Jaffe sum rule for proton, result strongly connected. This possibility finds particular evidence from the phenomenological observation that the relation $\Delta u = 2\tilde{F} + u - d - 1$ seems well satisfied by parton distributions.

1 Introduction

The experimental results on deep inelastic scattering (DIS) are always an inexhaustible source for deeper insight in the nucleon structure. Among them, the violation of well established sum rules represent the relevant starting point to unveil the mechanisms which rule the parton physics.

This consideration has inspired a recent series of papers, which starting from an old idea of Niégawa and Sasaki [1] and Field and Feynman [2], have focused the role played by Pauli exclusion principle on the quark/parton distributions inside nucleons [3]–[7]. In this framework, by virtue of the fermionic statistics, the violation of the Gottfried sum rule [8] and the Ellis–Jaffe sum rule for the proton [9] are related. Interestingly, this connection has also been observed in a more general framework by using standard parameterizations for parton distributions [10]–[12].

Moreover, the statistical inspired approach to the parton distributions has suggested a parameterization of quark/gluon distributions in terms of Fermi–Dirac/Bose–Einstein statistical functions. Remarkably, one obtains a satisfactory description of the experimental data of DIS in terms of few free parameters [4]. The analysis has then been improved [5] by adding an extra contribution to the *statistical* term of parton distributions, dominating in the small x region, the so called *liquid* component, with Pomeron–like quantum numbers.

There are several motivations for further work. The first one is the necessity of considering the polarized data with deuteron target at SLAC (E143) [13] and at CERN (SMC) [14]. These measurements, differently from the data obtained on neutron target at SLAC (E142) [15], seem to be consistent with Bjorken (Bj) sum rule [16] when QCD corrections are taken into account.

The second reason is to consider sets of data corresponding to the same Q^2 . In this respect, we choose for Q^2 the values 3 and 10 $(GeV/c)^2$, at which E143 and SMC are performed. Indeed, in the previous analysis the data used for xF_3 and on $F_2^p(x)$ ($F_2^n(x)$) were taken at slightly different Q^2 (3 and 4 $(GeV/c)^2$), and moreover one tried to fit the experimental results of $xg_1^p(x)$ corresponding to $Q^2 = 3$ $(GeV/c)^2$ and 10 $(GeV/c)^2$ by means of a single function, since they did not differ too much. Finally, for $xg_1^n(x)$ the

data were at $Q^2 = 2 \text{ (GeV/c)}^2$.

The third reason is to explore the possibility of gluons and/or strange quark polarization, which have been advocated to explain the defect in the Ellis–Jaffe (EJ) sum rule [9] for the proton in a framework consistent with the Bj sum rule.

Concerning the very important issue of testing the Bjorken sum rule, we want to stress the difficulty to evaluate the small x contribution, where the measured cross section has to be divided by x . In this respect, it would be helpful to know the small x behaviour of $g_1^p(x) - g_1^n(x)$. In the approach based on statistical functions this behaviour is given by the function $f(x)$ [5], which is also related to $F_2^p(x) - F_2^n(x)$ and $xF_3(x)$, occurring in the Gottfried and Gross Llewellyn–Smith sum rule [17], respectively. Since these quantities are measured more precisely than the g_1 ’s, $f(x)$ is practically determined by the unpolarized structure functions. Once $f(x)$ and the parameter \bar{x} are established [4, 5], the polarized structure function $g_1^p(x) - g_1^n(x)$ depends only on the *thermodynamical potentials* [4, 5] of quarks with definite spin. In practice, we have only one free parameter for each quark, since the sum $p^\uparrow(x) + p^\downarrow(x)$ is fixed by the unpolarized structure functions. In this way, we are able to obtain from the data the values of the parameters and an evaluation of the Bj sum rule less dependent on the large errors of the experimental data at small x .

We consider the data at $Q^2 = 3 \text{ (GeV/c)}^2$ and 10 (GeV/c)^2 as independent, without relating them by the evolution equations [18]. In principle, one should test whether, starting from quantum statistical distributions at a given Q^2 one gets the same form for the distributions at higher Q^2 , apart from some changes for the parameters. Practically, one has enough flexibility in our parameterization to reproduce the changes induced by the evolution equations, which bring to a narrowing of the parton distributions and of the structure functions.

The possibility that the evolution equations should be modified to take into account the statistical properties of partons has been studied, within the approximation to consider for parton momenta the longitudinal degree of freedom only [19]. The very important role of transverse degrees of freedom, however, demands that they should be taken into account in a model aiming to be realistic.

The paper is organized as follows, in the second section we give a brief review of the role of Pauli principle to explain some features of deep inelastic scattering (DIS) data. Section

three is devoted to describe the experimental results used for the numerical analysis. The results of the fit performed are shown in section four and finally, in section five we give our conclusions.

2 The Pauli principle and the structure functions

In the usual description for the deep inelastic phenomena, the quark/partons inside the nucleons are seen, in the infinitum momentum frame, as an ensemble of free particles which incoherently interact with the electroweak probe. In this scenario, no statistical effects are considered since they would depend on the overlapping of the quark wave functions.

A role of Pauli principle has been advocated to understand the defect in the Gottfried sum rule [8], and in the Ellis–Jaffe sum rule for the proton [9].

According to the Gottfried sum rule, one gets

$$I_G \equiv \int_0^1 \frac{dx}{x} [F_2^p(x) - F_2^n(x)] = \frac{1}{3} + \frac{2}{3} \int_0^1 dx [\bar{u}(x) - \bar{d}(x)] = \frac{1}{3} \quad , \quad (1)$$

where the last equality holds in the limit of $SU(2)_I$ -symmetric sea ($\bar{d} = \bar{u}$). The experimental measurement of I_G , by NMC [20], gives

$$I_G = 0.235 \pm 0.026 \quad , \quad (2)$$

which implies, assuming the validity of Adler sum rule [21], a strong violation of the isospin invariance of sea quarks

$$\bar{d} - \bar{u} = 0.15 \pm 0.04 \quad , \quad u - d = 0.85 \pm 0.04 \quad . \quad (3)$$

As far as the Ellis–Jaffe sum rule is concerned [9], for the proton it reads [22]

$$\begin{aligned} \Gamma_1^p &\equiv \int_0^1 dx g_1^p(x) = \int_0^1 dx \left[\frac{2}{9}(\Delta u(x) + \Delta \bar{u}(x)) + \frac{1}{18}(\Delta d(x) + \Delta \bar{d}(x)) \right. \\ &\quad \left. + \Delta s(x) + \Delta \bar{s}(x) \right) - \frac{\alpha_s(Q^2)}{6\pi} \Delta G(x) \Big] = \frac{\tilde{F}(Q^2)}{2} - \frac{\tilde{D}(Q^2)}{18} \quad , \end{aligned} \quad (4)$$

where the parameters $\tilde{F}(Q^2)$ and $\tilde{D}(Q^2)$ are given, up to the third order in $\alpha_s(Q^2)$, by the following expressions [23]

$$\tilde{F}(Q^2) = F - \frac{\alpha_s(Q^2)}{5\pi} \left(3F + \frac{2}{3}D \right) - \left(\frac{\alpha_s(Q^2)}{\pi} \right)^2 (2.092 F + 0.496 D)$$

$$- \left(\frac{\alpha_s(Q^2)}{\pi} \right)^3 4.044 (2 F + D) \quad , \quad (5)$$

$$\begin{aligned} \tilde{D}(Q^2) &= D - \frac{\alpha_s(Q^2)}{5\pi} \left(2 F + \frac{13}{3} D \right) - \left(\frac{\alpha_s(Q^2)}{\pi} \right)^2 (1.488 F + 3.084 D) \\ &- \left(\frac{\alpha_s(Q^2)}{\pi} \right)^3 4.044 (3 F + 4 D) \quad . \end{aligned} \quad (6)$$

Note that the last equality of Eq. (4) is obtained by neglecting the polarization of strange quarks and gluons. By using the values of F and D determined in Ref. [24]

$$F = 0.46 \pm 0.01 \quad , \quad D = 0.79 \pm 0.01 \quad , \quad (7)$$

one gets from (4): $\Gamma_1^p = .161 \pm .007$ at $Q^2 = 3 \text{ (GeV/c)}^2$ ($\alpha_s(3 \text{ (GeV/c)}^2) = 0.35 \pm 0.05$), and $\Gamma_1^p = 0.169 \pm .005$ at $Q^2 = 10 \text{ (GeV/c)}^2$ ($\alpha_s(10 \text{ (GeV/c)}^2) = .27 \pm .02$). These two quantities have been measured by E143 [25] and SMC [26] respectively, and result to be $\Gamma_1^p = 0.127 \pm 0.004 \pm 0.010$ at $Q^2 = 3 \text{ (GeV/c)}^2$ and $\Gamma_1^p = 0.136 \pm 0.011 \pm 0.011$ at $Q^2 = 10 \text{ (GeV/c)}^2$. The disagreement between the theoretical predictions and the experimental data, by virtue of Eq.(4), is typically explained in terms of a relevant polarization of strange quarks and/or gluons. As far as the strange quarks are concerned, since their polarization cannot exceed the less divergent part of the unpolarized distribution [27, 28] they cannot explain the EJ results, whereas the gluons due to the suppression factor $\alpha_s/6\pi$ need very strong polarization to be effective. This leads to a very unnatural scenario, in which the relevant gluon polarization has to be compensated by a strong angular orbital momentum of the partons. Furthermore, if we admit such a large anomaly contribution to explain the EJ sum rule on proton it would imply the dominance at low x of $\Delta G(x)$ over the other parton polarizations, and thus one would expect for $g_1^p(x)$ and $g_1^n(x)$ the same behaviour at low x by virtue of the isoscalar nature of gluons. This would contradict the trend, shown by the experimental data of SMC on proton [26] and deuteron [14], of a different behaviour at low x for $g_1^p(x)$ and $g_1^d(x)$.

Interestingly, the defects in the two sum rules may be easily explained in terms of the fermionic nature of quarks. In fact, the violation of the Gottfried sum rule can be understood by following the idea of Niégawa and Sasaki [1] and Field and Feynman [2], that Pauli principle disfavours the production of $u\bar{u}$ pairs in the proton with respect to $d\bar{d}$, since it contains two valence u quarks and only one d . For the same reason, the

violation of Ellis–Jaffe sum rule for proton may be explained by observing that at high x the $u^\uparrow(x)$ is the dominating parton distribution in the proton and again Pauli principle would disfavour contributions from the sea to u^\uparrow .

Information on the parton distributions can be obtained from their first momenta. Indeed at $Q^2 = 0$, the axial couplings of the baryon octet are fairly described in terms of the valence quarks

$$u_{val}^\uparrow = 1 + F \quad , \quad u_{val}^\downarrow = 1 - F \quad , \quad (8)$$

$$d_{val}^\uparrow = \frac{1 + F - D}{2} \quad , \quad d_{val}^\downarrow = \frac{1 - F + D}{2} \quad . \quad (9)$$

Thus, by using the experimental values for F and D [24]

$$u_{val}^\uparrow \simeq \frac{3}{2} \simeq u_{val}^\downarrow + d_{val}^\uparrow + d_{val}^\downarrow \quad . \quad (10)$$

This result on the abundances of the *valence* quarks, suggests to assume a similar relation for the parton distributions [3]. The leading idea, the so-called *shape–abundance* correlation, is that to more abundant partons correspond broader distribution functions, as stated from the Pauli principle. This assumption, which is a key property of the Fermi–Dirac distribution functions, can be tested by comparing the shapes of $u^\uparrow(x)$ with the ones of the other partons.

Indeed, one can observe that the behaviour at high x of $F_2^n(x)/F_2^p(x)$ [20], which experimentally tends to $\approx 1/4$, indicates the dominance of the u quarks, and in addition, the study of polarized $g_1^p(x)$ shows that at high x the partons with spin parallel to the proton dominate. In conclusion, at high x , the most abundant parton, u^\uparrow , dominates according to the already mentioned correlation shape–abundance.

As a consequence of this analysis, the Pauli principle seems to play a fundamental role in the DIS phenomena. Thus, in this framework it is natural to assume Fermi–Dirac distributions in the variable x for the quark partons [4, 5]

$$p(x) = f(x) \left[\exp \left(\frac{x - \tilde{x}(p)}{\bar{x}} \right) + 1 \right]^{-1} \quad , \quad (11)$$

where $f(x)$ is a weight function, \bar{x} plays the role of the temperature and $\tilde{x}(p)$ is the *thermodynamical potential* of the parton p , identified by its flavour and spin direction.

Analogously, for the gluons one should have

$$G^{\uparrow(\downarrow)}(x) = \frac{8}{3} f(x) \left[\exp \left(\frac{x - \tilde{x}(G^{\uparrow(\downarrow)})}{\bar{x}} \right) - 1 \right]^{-1} \quad . \quad (12)$$

The factor $8/3$ in (12) is just the ratio of the colour degeneracies for gluons and quarks. As far as the weight function $f(x)$ is concerned, it contains the information on the density of states for quarks and gluons inside the nucleon in the $P_z = \infty$ frame of reference. Nevertheless, it has to vanish at $x = 1$, and one should recover the usual parameterization for parton distributions when the statistical effects are negligible, hence we assume for it the usual form

$$f(x) = A x^\alpha (1-x)^\beta \quad , \quad (13)$$

where A , α and β are free parameters. Indeed, the expressions (11) and (12), assumed for quarks and gluons, are not able to recover the typical behaviour of the distribution functions at low x . In fact, the most divergent part of distributions is expected on general grounds to be equal for the different partons, at least in the limit of flavour symmetry, and hence it does not contribute to the sum rules, but affects other DIS observables. In order to disentangle, this divergent term from the total distribution function we add a *liquid* unpolarized component for the light quark-partons (u , d and their antiparticles) [5]

$$f_L(x) = (A_L/2) x^{\alpha_L} (1-x)^{\beta_L} \quad , \quad (14)$$

and the same x dependence, but with a different normalization for s and \bar{s} .

3 The experimental data

In a previous paper [5] the above analysis to determine the parton distributions in the *statistical inspired approach*, was performed by choosing sets of experimental data obtained at different Q^2 . In particular, as already stated in the introduction, the experimental results for xF_3 [29], and $F_2^p(x)$, $F_2^n(x)$ [20] were taken at slightly different Q^2 , 3 and 4 $(GeV/c)^2$, respectively. For the polarized function $g_1^p(x)$ one also tried to describe both data at $Q^2 = 3$ [25] and 10 $(GeV/c)^2$ [26] with the same function. Nevertheless, even in this approximation, due to the smooth dependence of the DIS observables on the Q^2 in the range 3 – 10 $(GeV/c)^2$, one found a good agreement between the experimental results and the theoretical predictions [5].

In the following analysis we will use sets of data which correspond to the same values of Q^2 . In particular we will perform our fit for the values of $Q^2 = 3$ $(GeV/c)^2$, and 10 $(GeV/c)^2$, corresponding to the measurements of $g_1^p(x)$ and $g_1^d(x)$ by E143 [13, 25], and

SMC [14, 26], respectively. For the same values of Q^2 , we will also analyze the unpolarized data on $xF_3(x)$, $F_2^p(x)$ and $F_2^n(x)$.

As long as $xF_3(x)$ is concerned, CCFR [29] gives directly the data at $Q^2 = 3 \text{ (GeV/c)}^2$, whereas to get the results at $Q^2 = 10 \text{ (GeV/c)}^2$ we use a linear interpolation in $\log Q^2$. For the ratio $F_2^n(x)/F_2^p(x)$, we start from the data at $Q^2 = 4 \text{ (GeV/c)}^2$ reported in Ref. [20] and get the values at $Q^2 = 3$ and 10 (GeV/c)^2 , by means of the formula

$$\frac{F_2^n(x, Q^2)}{F_2^p(x, Q^2)} = \frac{F_2^n(x, 4 \text{ (GeV/c)}^2)}{F_2^p(x, 4 \text{ (GeV/c)}^2)} + B(x) \log \left[\frac{Q^2}{4 \text{ (GeV/c)}^2} \right] \quad , \quad (15)$$

written in Ref. [30], where $B(x)$ is also given.

For this parameterization the systematic errors are evaluated according to Ref. [20], whereas the statistical ones are taken from the measurements at $Q^2 = 4 \text{ (GeV/c)}^2$ [20]. Finally, the data on $F_2^p(x)$ are taken from Hera, SLAC and NMC [20], [31], [32].

We will also take into account the NA51 result for the Drell–Yan processes on proton and deuteron targets [33], which depends mainly on the ratio $\bar{u}(.18)/\bar{d}(.18)$ and provides the measurement for this ratio $0.51 \pm 0.04 \pm 0.05$, and as far as the gluons are concerned, the unpolarized theoretical distribution, which we impose to carry the fraction of proton momentum not carried by the quark partons, will be compared with the experimental results reported in [34]–[36].

4 Comparison with experiment

As in Ref. [5] we take for quark/parton distributions the following expression

$$p(x) = f_L(x) + Ax^\alpha(1-x)^\beta \left[\exp \left(\frac{x - \tilde{x}(p)}{\bar{x}} \right) + 1 \right]^{-1} \quad . \quad (16)$$

The parameters A_L , α_L and β_L occurring in the definition of $f_L(x)$ (see Eq. (14)), define the low x behaviour of parton distributions, independently of the parton specie, the so-called *liquid* term, whereas A , α and β fix the weight function in the *gas* term. Finally, the statistical functions, which depend on the parton are simply defined by an *universal temperature* parameter, \bar{x} , and by the *thermodynamical potentials* $\tilde{x}(p)$. Note that, p stands for partons with given flavour and polarization. For the strange quarks, we take for their unpolarized structure functions the following expression

$$s(x) = \bar{s}(x) = A_s \frac{\bar{u}(x) + \bar{d}(x)}{2} \quad , \quad (17)$$

with $A_s = .475$ according to Ref. [37]. Here, we also allow for polarized gluon distributions

$$G^{\uparrow(\downarrow)}(x) = \frac{8}{3} A x^\alpha (1-x)^\beta \left[\exp \left(\frac{x - \tilde{x}(G^{\uparrow(\downarrow)})}{\bar{x}} \right) - 1 \right]^{-1}. \quad (18)$$

Should we consider also the *liquid* component for gluons, the momentum fraction carried by the gas component should be smaller, giving rise to smaller *thermodynamical* potentials $\tilde{x}(G^{\uparrow(\downarrow)})$. However, since only $\Delta G(x)$ appears in the structure functions, the error implied by neglecting the *liquid* gluon component, which is expected to carry only a small fraction of the total momentum, it is not relevant for the issue of deciding is a Bose/Einstein gluon contribution may solve the spin crisis.

Of course, to get a fair description of the gluon distributions, one should have also a *liquid* gluon component. Since, the low x gluon data are at $Q^2 = 20 \text{ (GeV/c)}^2$ [34]–[36], while we try to reproduce the structure functions at $Q^2 = 3$ and 10 (GeV/c)^2 , where $g_1^p(x)$ and $g_1^d(x)$ are measured, a description of $G(x)$ goes beyond the purpose of this work.

The large negative values found in Ref. [5] for $\tilde{x}(\bar{u})$ and $\tilde{x}(\bar{d})$ imply negligible effects of Pauli principle for the \bar{q} 's (the levels are very little occupied) and when we can neglect 1 in the denominator of (16) the distribution become Boltzman-like and with the same x dependence. Thus, it is a good approximation within our general approach to put

$$\Delta \bar{u}(x) \simeq k_u [\bar{u}(x) - 2f_L(x)] \quad , \quad (19)$$

$$\Delta \bar{d}(x) \simeq k_d [\bar{d}(x) - 2f_L(x)] \quad , \quad (20)$$

$$\Delta s(x) + \Delta \bar{s}(x) \simeq k_s [s(x) + \bar{s}(x) - 1.9f_L(x)] \quad , \quad (21)$$

with $|k_u|, |k_d|, |k_s| \leq 1$. We tried, in our approach, several options to see how much the different solutions proposed for spin crisis are supported by data. In Tables I.a and I.b, we report for four different options, the values of normalized χ^2 , Δq_i and $\Delta \bar{q}_i$ (with $i = u, d, s$) and ΔG_i , and moreover the corresponding evaluations of the EJ and Bj sum rules (with in brackets the expected values up to the third order in QCD corrections) for $Q^2 = 3$ and 10 (GeV/c)^2 , respectively.

The following remarks are then in turn.

a) To summarize the results of Tables I.a and I.b one can observe that at $Q^2 = 3 \text{ (GeV/c)}^2$

- $.640 \leq \Delta u + \Delta \bar{u} \leq .674$ to be compared with the QCD prediction $.782$ up to α_s^3 ;

- $-.300 \leq \Delta d + \Delta \bar{d} \leq -.260$ versus the QCD prediction $-.238$;
- finally, for the Bj sum rule one gets $.155 \leq (\Delta u + \Delta \bar{u} - \Delta d - \Delta \bar{d})/6 \leq .157$ to be compared with $.170$.

The same quantities for $Q^2 = 10 \text{ (GeV/c)}^2$ result to be

- $.670 \leq \Delta u + \Delta \bar{u} \leq .730$ to be compared with $.826$ from QCD;
- $-.290 \leq \Delta d + \Delta \bar{d} \leq -.183$ versus $-.268$;
- $.156 \leq (\Delta u + \Delta \bar{u} - \Delta d - \Delta \bar{d})/6 \leq .160$ to be compared with $.183$.

Thus, in both cases $\Delta u + \Delta \bar{u}$ is smaller than the QCD result, while only at $Q^2 = 3 \text{ (GeV/c)}^2$ we have a $\Delta d + \Delta \bar{d}$ more negative than the QCD value. It is somehow surprising the result found for the Bj sum rule at $Q^2 = 10 \text{ (GeV/c)}^2$. We find a defect, while from its own data SMC gets an excess (consistent within the errors with the predicted value). The origin of this discrepancy can be understood as a consequence of our assumption of a common behaviour at low x of the parton component contributing to the sum rules. In this way, in fact, we constrain the contribution to the polarized sum rule to have the same behaviour in the $x \rightarrow 0$ limit of the unpolarized ones. The value found for $\bar{x} \gtrsim .2$ gives a very smooth dependence at small x for the ratio of the different parton distributions. In fact, in this x region we are unable to reproduce the measurements of $xg_1^p(x)$, and the fast decrease to negative values of $xg_1^d(x)$. The Bose–Einstein form chosen for the gluons enhances their contributions at low x , but cannot account for a different behaviour of $xg_1^p(x)$ and $xg_1^n(x)$ in that limit for its isoscalar nature. In fact our fit, with almost half the contribution to the χ^2 coming from deuteron data despite their large errors, is unable to reproduce these typical features of SMC data.

b) The possibility to have $\Delta \bar{d} \neq 0$ leads to very unphysical situations, namely, very negative Δd , partially compensated by positive $\Delta \bar{d}$ at $Q^2 = 3 \text{ (GeV/c)}^2$, and small positive Δd with larger negative $\Delta \bar{d}$ at $Q^2 = 10 \text{ (GeV/c)}^2$. These results come from the difficulty of the fit procedure to disentangle in $\Delta \bar{d} + \Delta d$ the single two contributions, which in the previous paper led us to assume $\Delta \bar{d} = 0$. Since, when we allow for $\Delta \bar{d} \neq 0$, the sum $\Delta \bar{d} + \Delta d$, is more negative than for $\Delta \bar{d} = 0$ at $Q^2 = 3 \text{ (GeV/c)}^2$ and less negative at $Q^2 = 10 \text{ (GeV/c)}^2$, we think it is better to assume also in the present analysis $\Delta \bar{d} = 0$.

The sum $\Delta u + \Delta \bar{u}$ does not change so much when we take $\Delta \bar{u} \neq 0$. Finally, one can observe that the strange quark polarization ($\Delta s + \Delta \bar{s}$) comes out positive when $\Delta G \neq 0$, and negative, except a case with $\Delta \bar{d} = 0$ at $Q^2 = 3 \text{ (GeV/c)}^2$, for $\Delta G = 0$ as it is expected to give a relevant negative contribution to the EJ sum rule for the proton. However, with the only exclusion of a case with $\Delta \bar{d} \neq 0$ ($\Delta s + \Delta \bar{s}$) gives a small contribution ($-.0045$) to the EJ sum rules and the corresponding fits practically give the same value to the Bj sum rule as the ones with $(\Delta s + \Delta \bar{s}) = 0$.

c) Let us consider finally the role of ΔG , which gives the most accepted solution of the *spin crisis* [22]. We find always positive values for ΔG , which implies negative contributions to the EJ sum rules, but its presence does not modify the Bj sum rule, which becomes smaller at $Q^2 = 3 \text{ (GeV/c)}^2$, and even more at 10 (GeV/c)^2 than the predicted value (with QCD corrections up to the third order in α_s). We understand this behaviour as a result of the very strong restrictions on our description of $\Delta G(x)$. According to Eq. (18), in fact, the function $f(x)$, which appears in the parameterization of the gluon distributions, is determined by the unpolarized data. Moreover, since the Bose–Einstein factor $[\exp(x - \tilde{x}(G)/\bar{x}) - 1]^{-1}$ enhances the small x region, $\Delta G(x)$ has a very little overlap with $\Delta u(x)$ and $\Delta d(x)$ and consequently the value of ΔG has little influence on Δu and Δd . The relatively smooth behaviour at low x seen by E143, as well as the different behaviour in the same x region of $xg_1^p(x)$ and $xg_1^d(x)$ seen by SMC, hardly to be described by a $I = 0$ term as the gluon contribution, do not ask for an important role of the anomaly for the description of the polarized structure functions studied.

d) The values found for the exponents α_L , -1.18 at $Q^2 = 3 \text{ (GeV/c)}^2$ and -1.28 at $Q^2 = 10 \text{ (GeV/c)}^2$, confirm our assumption that *liquid* term should not contribute to the quark parton model sum rules, which otherwise would not converge.

To reach an idea of the quality of the fits found, as well as the effect of the anomaly contributions, we report in Tables II.a and II.b the parameters and the gas abundances for partons, found with $\Delta \bar{q}_i = 0$ and with/without $\Delta G(x)$ at $Q^2 = 3$, and 10 (GeV/c)^2 , and compare them with the results of a previous paper [5]. Figures 1.a–5.a and 1.b–5.b show our theoretical predictions versus the experimental data, for $F_2^n(x)/F_2^p(x)$, $F_2^p(x)$, $xF_3(x)$, $xg_1^p(x)$, and $xg_1^d(x)$ corresponding to $Q^2 = 3$ and $Q^2 = 10 \text{ (GeV/c)}^2$ respectively, for the fits with $\Delta G = 0$ (solid line) and $\Delta G \neq 0$ (dashed line) reported in Tables II.a and

II.b. For the same choices of parameters, the predictions for $xg_1^n(x)$ at $Q^2 = 3 \text{ (GeV/c)}^2$ are compared with the measurements at $Q^2 = 2 \text{ (GeV/c)}^2$ by E142 [15] in Figure 6., and in Figure 7.a , 7.b the predictions for unpolarized gluon distributions are plotted versus the experimental results [34]–[36]. Note that, as already stated at the beginning of the section, the lack of agreement at $x \lesssim .1$ shows the necessity of a *liquid* component also for the gluons. Finally, in Figure 8., the ratios $u^\uparrow(x)/d(x)$ and $u^\downarrow(x)/d(x)$ are plotted for the choice of parameters of Table II.a and II.b corresponding to $\Delta G = 0$.

5 Conclusions

As we expected, the narrowing of the parton distributions implied by the evolution equations [18] is easily realized with a slight increasing of the parameters α and α_L , responsible for the low x behaviour of the gas and *liquid* distributions respectively, and with a slight decreasing of the *thermodynamical* potentials. Indeed, the shape-abundance correlation, so clearly indicated by data for the u^\uparrow parton, may not be washed out by the logarithmic corrections from $Q^2 = 3$ to 10 (GeV/c)^2 .

The good description we get for $F_2^p(x)$, $F_2^n(x)$ and $xF_3(x)$, confirms that the correlation shape–abundance, peculiar of our scheme based on Pauli principle, is obeyed by the parton distributions.

The connection between the defects in the Gottfried and Ellis–Jaffe sum rules based on Pauli principle finds support on the fact that the relationship

$$\Delta u \simeq 2\tilde{F} + u - d - 1 \quad , \quad (22)$$

is rather well satisfied by the parton distributions found also with $\Delta G \neq 0$.

It is also instructive to compare the behaviour of the ratios $u^\uparrow(x)/d(x)$ and $u^\downarrow(x)/d(x)$ of our distributions, described in Figure 8. The first ratio, in fact, is a rapidly increasing function of x , whereas the second one is almost constant $\approx .5$, in good agreement with the expected value $1 - F$.

The presence of a defect in the Bj sum rule also for the fit in which we allow for $\Delta G \neq 0$, arises from the specific properties of our Bose–Einstein description for gluons. In particular, the ratio $\Delta G(x)/G(x)$ results to be large at small x where the difference between the small negative values of $\tilde{x}(G^\uparrow)$ and $\tilde{x}(G^\downarrow)$ is relevant, and it is rapidly decreasing to about

$\tanh(\tilde{x}(G^\uparrow) - \tilde{x}(G^\downarrow)/2\bar{x})$ at large x . As a consequence of the modest overlap of $\Delta G(x)$ and $\Delta u(x)$ and $\Delta d(x)$, Δu and Δd are slightly influenced by the value of ΔG .

We would like to thank Drs. Gianpiero Mangano, Ofelia Pisanti and Pietro Santorelli for useful discussions and valuable comments.

References

- [1] A. Niégawa and K. Sasaki, Prog. Theor. Phys. **54** (1975) 192.
- [2] R.D. Field and R.P. Feynman, Phys. Rev **D15** (1977) 2590.
- [3] F. Buccella and J. Soffer, preprint CPT-92/P/2706; Mod. Phys. Lett. **A8** (1993) 225; Europh. Lett. **24** (1993) 165; Phys. Rev. **D48** (1993) 5416.
- [4] C. Bourrely, F. Buccella, G. Miele, G. Migliore, J. Soffer and V. Tibullo, Zeit. Phys. **C62** (1994) 431.
- [5] F. Buccella, G. Miele, G. Migliore and V. Tibullo, Zeit. Phys. **C68** (1995) 631.
- [6] C. Bourrely, J. Soffer, Phys. Rev. **D51** (1995) 2108.
- [7] C. Bourrely, J. Soffer, Nucl. Phys. **B445** (1995) 341.
- [8] K. Gottfried, Phys. Rev. Lett. **18** (1967) 1174.
- [9] J. Ellis and R.L. Jaffe, Phys. Rev. **D9** (1974) 1444; *erratum* **D10** (1974) 1669.
- [10] F. Buccella, O. Pisanti, P. Santorelli and J. Soffer, hep-ph/9507251, to appear in Nuovo Cimento A.
- [11] C. Bourrely, F. Buccella, O. Pisanti, P. Santorelli and J. Soffer, DSF-T-17/96, CPT-96/PE.3327, hep-ph/9604204.
- [12] O. Pisanti, Ph.D. thesis, unpublished.
- [13] K. Abe et al. (E143 collaboration), Phys. Rev. Lett. **75** (1995) 25.
- [14] D. Adams et al. (SMC collaboration), Phys. Lett. **B357** (1995) 248.
- [15] P.L. Anthony et al. (E142 collaboration), Phys. Rev. Lett. **71** (1993) 959.
- [16] J.D. Bjorken, Phys. Rev. **148** (1966) 1467; Phys. Rev. **D1** (1970) 1376.
- [17] D. Gross and C.H. Llewellyn-Smith, Nucl. Phys. **B14** (1969) 337.

- [18] G. Altarelli and G. Parisi, Nucl. Phys. **B126** (1977) 298; V.N. Gribov and L.N. Lipatov, Sov. J. Nucl. Phys. **15** (1972) 438, 675; L.N. Lipatov, Sov. J. Nucl. Phys. **20** (1975) 94; Y.L. Dokshitzer, Sov. Phys. JETP, **46** (1977) 641.
- [19] G. Mangano, G. Miele and G. Migliore, Nuovo Cim. **A108** (1995) 867.
- [20] M. Arneodo et al. (NMC collaboration), Phys. Rev. **D50** (1994) R1.
- [21] S.L. Adler, Phys. Rev. **143** (1966) 1144.
- [22] G. Altarelli and G.G. Ross, Phys. Lett. **B212** (1988) 391; R.D. Carlitz, J.C. Collins and A.H. Mueller, Phys. Lett. **B214** (1988) 229.
- [23] J. Kodaira, S. Matsuda, K. Sasaki, and T. Uematsu, Nucl. Phys. **B159** (1979) 99; J. Kodaira, Nucl. Phys. **B165** (1979) 129; J. Kodaira, S. Matsuda, T. Muta, K. Sasaki, and T. Uematsu, Phys. Rev. **D20** (1979) 627; S.A. Larin and J.A.M. Vermaseren, Phys. Lett. **B259** (1991) 345; S.A. Larin, Phys. Lett. **B334** (1994) 192.
- [24] S.Y. Hsueh et al., Phys. Rev. **D38** (1988) 2056.
- [25] K. Abe et al. (E143 collaboration), Phys. Rev. Lett. **74** (1995) 346.
- [26] D. Adams et al. (SMC collaboration), Phys. Lett. **B329** (1994) 399.
- [27] G. Preparata and J. Soffer, Phys. Rev. Lett. **61** (1988) 1167; **62** (1989) 1213 (E).
- [28] G. Preparata, Ph. Ratcliffe and J. Soffer, Phys. Lett. **B273** (1991) 306.
- [29] W.C. Leung et al. (CCFR collaboration), Phys. Lett. **B317** (1993) 655.
- [30] P.Amaudruz et al., Nucl. Phys. **B371** (1992) 3.
- [31] B. Foster, preprint DESY 95-158, August 1995; G. Radl (H1 collaboration), preprint DESY 95-152D, April 1995.
- [32] R.G. Roberts and M.R. Whalley, J. Phys. G: Nucl. Part. Phys. **17** (1991) D1.
- [33] A. Baldit et al. (NA51 collaboration), Phys. Lett. **B332** (1994) 244.
- [34] P. Perge et al. (CDHSW collaboration), Zeit. Phys. **C49** (1991) 187.
- [35] M. Virchaux and A. Milsztajn, Phys. Lett. **B274** (1992) 221.
- [36] M. Arneodo et al. (NMC collaboration), Phys. Lett. **B309** (1993) 222.
- [37] A.O. Bazarko et al. (CCFR collaboration), Zeit. Phys. **C65** (1995) 189.

Table I.a

$Q^2 = 3$ (GeV/c) ²	$\Delta\bar{u} = \Delta G = 0$ $\Delta(s + \bar{s}) = 0$	$\Delta\bar{u} = 0$ $\Delta(s + \bar{s}) = 0$	$\Delta\bar{u} = 0$ $\Delta G = 0$	$\Delta(s + \bar{s}) = 0$	QCD predictions	Experimental data
Δu	.640	.660	.671	.612	.782	
$\Delta\bar{u}$	0.	0.	0.	.062		
Δd	-.300	-.270	-.263	-.260	-.238	
$\Delta(s + \bar{s})$	0.	0.	-.080	0.		
ΔG	0.	.40	0.	.94		
Γ_1^p	.126	.124	.130	.118	.161 ± .007	.127 ± .004 ± .010 [25]
Γ_1^n	-.031	-.031	-.026	-.039	-.009 ± .005	-.035 ± .016 [13, 25]
$\Gamma_1^p - \Gamma_1^n$.157	.155	.156	.157	.170 ± .009	.163 ± .010 ± .016 [13]
χ_{tot}^2/N	2.33	2.32	2.34	2.34		
χ_p^2/N	1.19	1.24	1.24	1.25		
χ_d^2/N	1.16	1.06	1.17	1.12		

Table I.b

$Q^2 = 10$ (GeV/c) ²	$\Delta\bar{u} = \Delta G = 0$ $\Delta(s + \bar{s}) = 0$	$\Delta\bar{u} = 0$ $\Delta(s + \bar{s}) = 0$	$\Delta\bar{u} = 0$ $\Delta G = 0$	$\Delta(s + \bar{s}) = 0$	QCD predictions	Experimental data
Δu	.670	.730	.703	.588	.826	
$\Delta\bar{u}$	0.	0.	0.	.138		
Δd	-.290	-.210	-.255	-.183	-.268	
$\Delta(s + \bar{s})$	0.	0.	-.081	0.		
ΔG	0.	1.5	0.	2.44		
Γ_1^p	.133	.129	.137	.117	.169 ± .005	.136 ± .011 ± .011 [26]
Γ_1^n	-.027	-.028	-.021	-.039	-.014 ± .004	-.062 ± .029 [14, 26]
$\Gamma_1^p - \Gamma_1^n$.160	.157	.158	.156	.183 ± .006	.199 ± .038[14]
χ_{tot}^2/N	1.21	1.17	1.23	1.12		
χ_p^2/N	.60	.89	.67	1.0		
χ_d^2/N	2.90	2.56	3.22	2.62		

Table II.a

Param. $Q^2 = 3$ (GeV/c) ²	Previous fit [5] ($\chi^2/N = 2.47$)		Present fit with only $\Delta u, \Delta d \neq 0$ ($\chi^2/N = 2.33$)		Present fit with only $\Delta u, \Delta d, \Delta G \neq 0$ ($\chi^2/N = 2.32$)	
A	$2.66^{+.09}_{-.08}$		$2.51 \pm .07$		$2.54 \pm .08$	
α	$-.203 \pm .013$		$-.231 \pm .012$		$-.231 \pm .011$	
β	$2.34^{+.05}_{-.06}$		$2.21 \pm .04$		$2.22 \pm .04$	
A_L	$.0895^{+.0107}_{-.0084}$		$.127^{+.016}_{-.013}$		$.128^{+.015}_{-.013}$	
α_L	$-1.19 \pm .02$		$-1.18^{+.03}_{-.02}$		$-1.18 \pm .02$	
β_L	$7.66^{+1.82}_{-1.59}$		$10.3^{+1.4}_{-1.3}$		$10.1^{+1.4}_{-1.3}$	
\bar{x}	$.235 \pm .009$	gas abund.	$.214 \pm .008$	gas abund.	$.223 \pm .011$	gas abund.
$\tilde{x}(u^\uparrow)$	$1.00 \pm .07$	$1.15 \pm .01$	$1.00 \pm .02$	$1.22 \pm .01$	$1.00 \pm .02$	$1.23 \pm .01$
$\tilde{x}(u^\downarrow)$	$.123 \pm .012$	$.53 \pm .01$	$.141 \pm .011$	$.58 \pm .01$	$.129^{+.014}_{-.015}$	$.57^{+.02}_{-.01}$
$\tilde{x}(d^\uparrow)$	$-.068^{+.021}_{-.024}$	$.33 \pm .03$	$-.029^{+.019}_{-.020}$	$.37^{+.02}_{-.03}$	$-.028 \pm .020$	$.38 \pm .03$
$\tilde{x}(d^\downarrow)$	$.200^{+.013}_{-.014}$	$.62 \pm .01$	$.211 \pm .011$	$.67 \pm .01$	$.196^{+.015}_{-.016}$	$.65 \pm .01$
$\tilde{x}(\bar{u}^\uparrow)$	$-.886 \pm .266$	$.015^{+.034}_{-.009}$	$-.522^{+.049}_{-.061}$	$.054^{+.019}_{-.017}$	$-.559^{+.057}_{-.075}$	$.052^{+.022}_{-.019}$
$\tilde{x}(\bar{u}^\downarrow)$	"	"	"	"	"	"
$\tilde{x}(\bar{d}^\uparrow)$	$-.460^{+.047}_{-.064}$	$.08^{+.03}_{-.02}$	$-.339^{+.032}_{-.040}$	$.12 \pm .04$	$-.366^{+.037}_{-.049}$	$.12^{+.05}_{-.04}$
$\tilde{x}(\bar{d}^\downarrow)$	"	"	"	"	"	"
$\tilde{x}(G^\uparrow)$	$-.067$	3.16	$-.067^{+.008}_{-.009}$	$2.9 \pm .4$	$-.069 \pm .09$	$3.0^{+.05}_{-.04}$
$\tilde{x}(G^\downarrow)$	"	"	"	"	$-.085^{+.015}_{-.019}$	$2.6^{+.06}_{-.05}$

Table II.b

Parameters $Q^2 = 10$ (GeV/c) ²	Present fit with only $\Delta u, \Delta d \neq 0$ ($\chi^2/N = 1.21$)		Present fit with only $\Delta u, \Delta d, \Delta G \neq 0$ ($\chi^2/N = 1.17$)	
A	2.04 ^{+0.12} _{−.21}		1.98 ^{+0.19} _{−.15}	
α	−.343 ^{+0.023} _{−.062}		−.376 ^{+0.046} _{−.036}	
β	2.29 ± .04		2.28 ^{+0.05} _{−.04}	
A_L	.104 ^{+0.027} _{−.012}		.108 ^{+0.021} _{−.016}	
α_L	−1.28 ^{+0.03} _{−.02}		−1.28 ^{+0.03} _{−.02}	
β_L	7.6 ^{+8.0} _{−1.0}		10.8 ^{+4.7} _{−4.0}	
\bar{x}	.252 ^{+0.012} _{−.035}	gas abund.	.247 ^{+0.029} _{−.021}	gas abund.
$\tilde{x}(u^\uparrow)$	1.00 ± .01	1.26 ± .11	1.00 ± .01	1.35 ^{+0.05} _{−.07}
$\tilde{x}(u^\downarrow)$.102 ^{+0.043} _{−.040}	.59 ^{+0.04} _{−.01}	.092 ^{+0.050} _{−.073}	.62 ^{+0.03} _{−.08}
$\tilde{x}(d^\uparrow)$	−.115 ^{+0.101} _{−.061}	.35 ^{+0.10} _{−.07}	−.051 ^{+0.064} _{−.093}	.44 ^{+0.06} _{−.11}
$\tilde{x}(d^\downarrow)$.142 ^{+0.047} _{−.034}	.64 ± .04	.111 ^{+0.044} _{−.064}	.65 ^{+0.02} _{−.07}
$\tilde{x}(\bar{u}^\uparrow)$	−1.0 ± .2	.015 ^{+0.022} _{−.011}	−.68 ± .18	.053 ^{+0.069} _{−.033}
$\tilde{x}(\bar{u}^\downarrow)$	"	"	"	"
$\tilde{x}(\bar{d}^\uparrow)$	−.492 ± .11	.10 ^{+0.11} _{−.07}	−.42 ± .10	.14 ^{+0.16} _{−.09}
$\tilde{x}(\bar{d}^\downarrow)$	"	"	"	"
$\tilde{x}(G^\uparrow)$	−.095 ^{+0.003} _{−.001}	3.29 ^{+1.25} _{−.064}	−.076 ^{+0.014} _{−.021}	4.3 ± 1.0
$\tilde{x}(G^\downarrow)$	"	"	−.121 ^{+0.033} _{−.063}	2.8 ± 1.2

Table captions

Table I.a For four different options, the values of normalized χ^2 , the parton polarizations, and the corresponding evaluations of Γ_1^p , Γ_1^n and $\Gamma_1^p - \Gamma_1^n$ are reported, versus the QCD predictions up to α_s^3 and the experimental data. The values correspond to $Q^2 = 3 \text{ (GeV/c)}^2$.

Table I.b The same quantities of Table I.a, are computed for $Q^2 = 10 \text{ (GeV/c)}^2$.

Table II.a The parameters and the gas abundances for partons, found with $\Delta\bar{q}_i = 0$ and with/without $\Delta G(x)$ at $Q^2 = 3 \text{ (GeV/c)}^2$ are reported and compared with the results of Ref. [5]. Note that, no antiquarks or strange quark polarization is assumed.

Table II.b The same quantities of Table II.a are shown for $Q^2 = 10 \text{ (GeV/c)}^2$.

Figure captions

Figure 1.a The prediction for $F_2^n(x)/F_2^p(x)$ at $Q^2 = 3 \text{ (GeV/c)}^2$ is plotted and compared with the experimental data [20, 30], the solid line and the dashed line corresponds to the fit with $\Delta G = 0$ and $\Delta G \neq 0$ of Table II.a, respectively. This notation is valid for all Figures 1.a-5.a, 6., and 7.a .

Figure 1.b The same quantity of Figure 1.a is plotted for $Q^2 = 10 \text{ (GeV/c)}^2$, the solid line and the dashed line corresponds to the fit with $\Delta G = 0$ and $\Delta G \neq 0$ of Table II.b, respectively. This notation is valid for all Figures 1.b-5.b, and 7.b .

Figure 2.a The prediction for $F_2^p(x)$ at $Q^2 = 3 \text{ (GeV/c)}^2$ is plotted and compared with the experimental data [31], [20] and [32].

Figure 2.b The same quantity of Figure 2.a is plotted for $Q^2 = 10 \text{ (GeV/c)}^2$.

Figure 3.a $xF_3(x)$ is plotted for $Q^2 = 3 \text{ (GeV/c)}^2$ and the experimental values are taken from [29].

Figure 3.b $xF_3(x)$ is plotted for $Q^2 = 10 \text{ (GeV/c)}^2$ and the experimental values are taken from [29].

Figure 4.a $xg_1^p(x)$ at $Q^2 = 3 \text{ (GeV/c)}^2$ is plotted and compared with the data [25].

Figure 4.b The same quantity of Figure 4.a corresponding to $Q^2 = 10 \text{ (GeV/c)}^2$ is plotted versus the experimental data [26].

Figure 5.a $xg_1^d(x)$ at $Q^2 = 3 \text{ (GeV/c)}^2$ is plotted and compared with the data [13].

Figure 5.b The same quantity of Figure 5.a corresponding to $Q^2 = 10 \text{ (GeV/c)}^2$ is plotted versus the experimental data [14].

Figure 6. $xg_1^n(x)$ at $Q^2 = 3 \text{ (GeV/c)}^2$ is plotted versus the experimental data at $Q^2 = 2 \text{ (GeV/c)}^2$ by E142 [15].

Figure 7.a The predictions for unpolarized gluon distribution at $Q^2 = 3 \text{ (GeV/c)}^2$ are reported versus the experimental results [34]–[36].

Figure 7.b The same quantity of Figure 7.a, but corresponding to $Q^2 = 10 \text{ (GeV/c)}^2$ is shown.

Figure 8. The solid line represents the ratio $u^\uparrow(x)/d(x)$, and the dashed one $u^\downarrow(x)/d(x)$, for the choice of parameters corresponding to the second column of Table II.a. The dashed-dotted line and the dotted one, represent the same quantities but corresponding to the first column of Table II.b .

Fig. 1.a

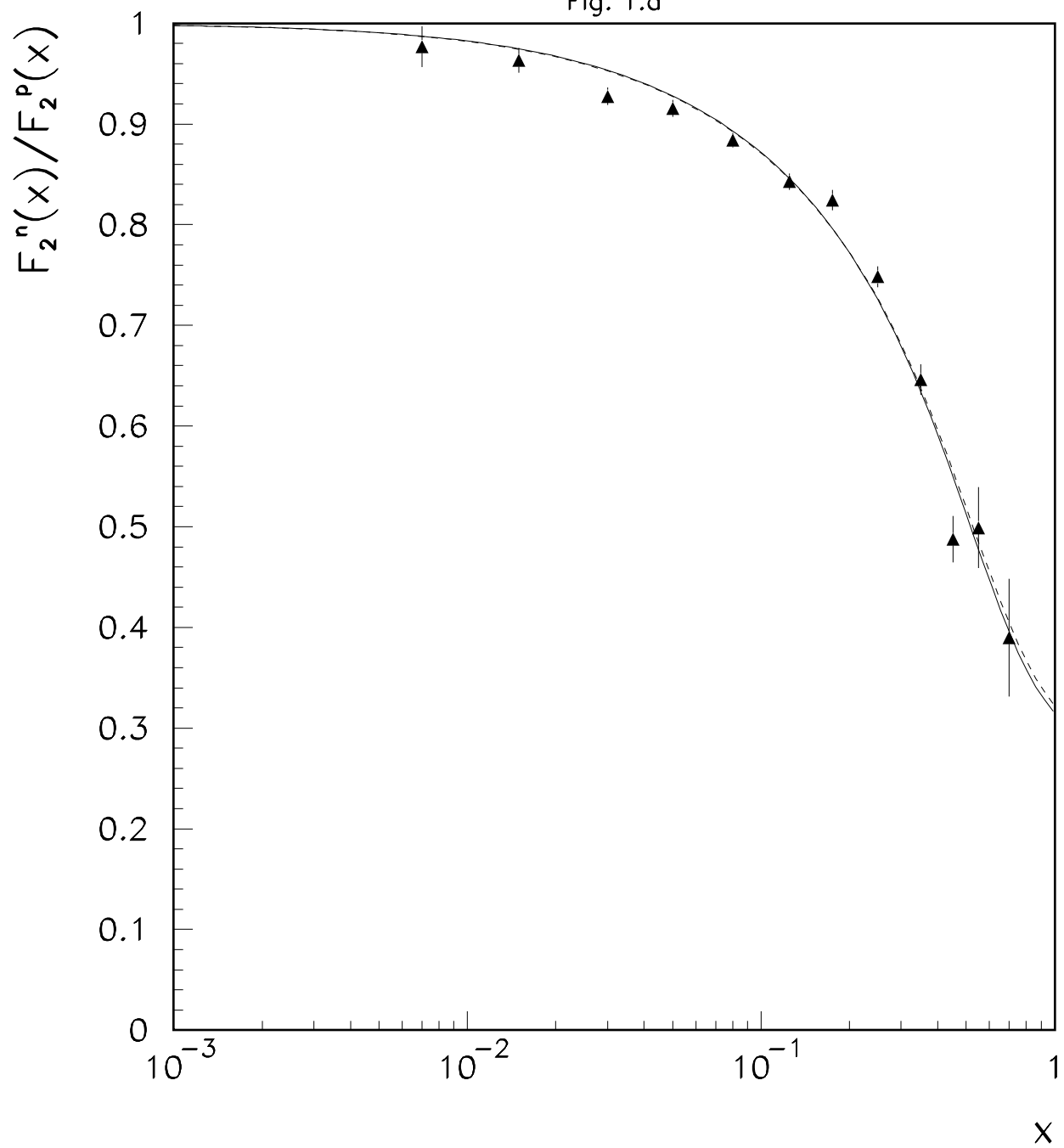


Fig. 1b

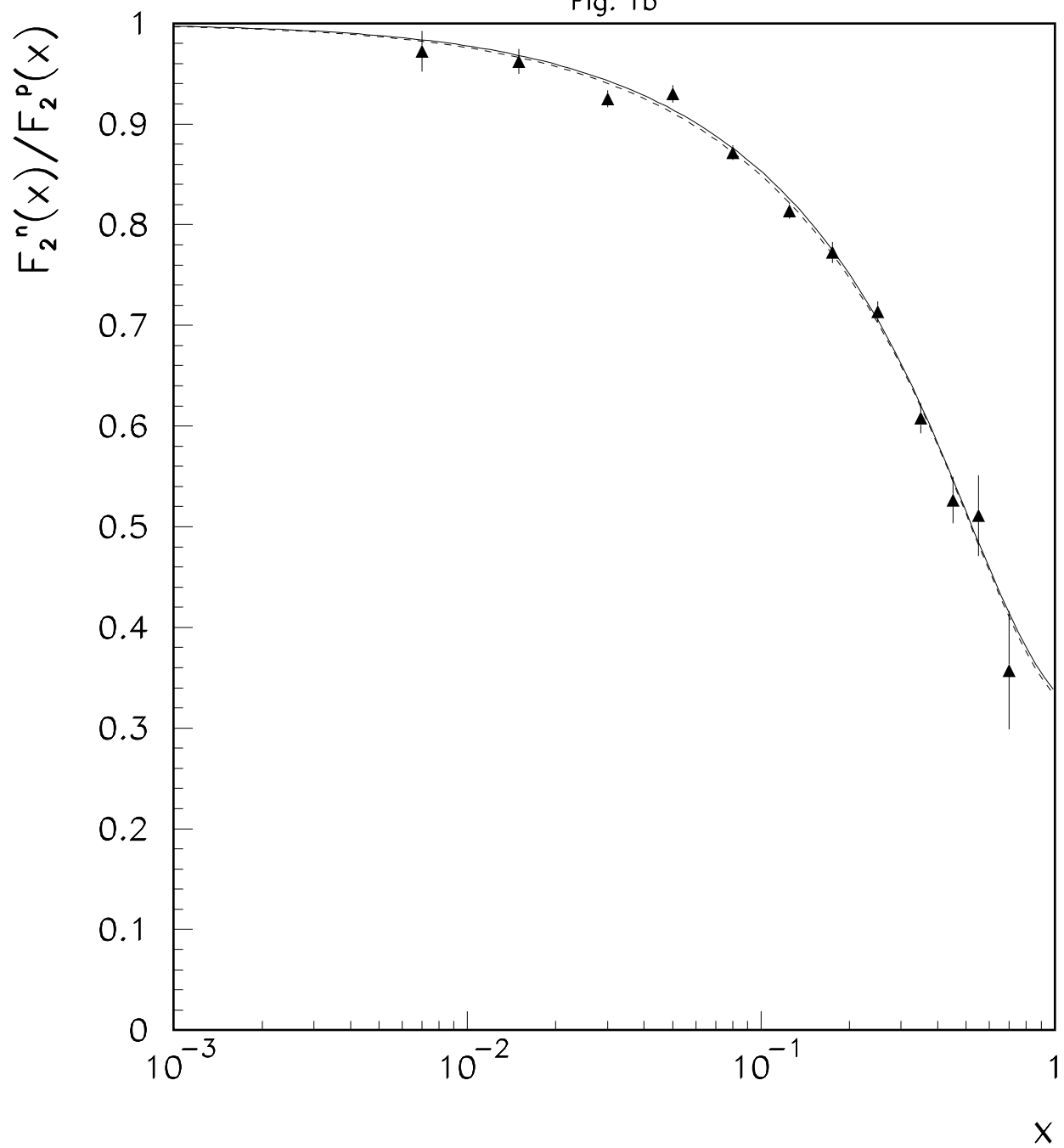


Fig. 2.a

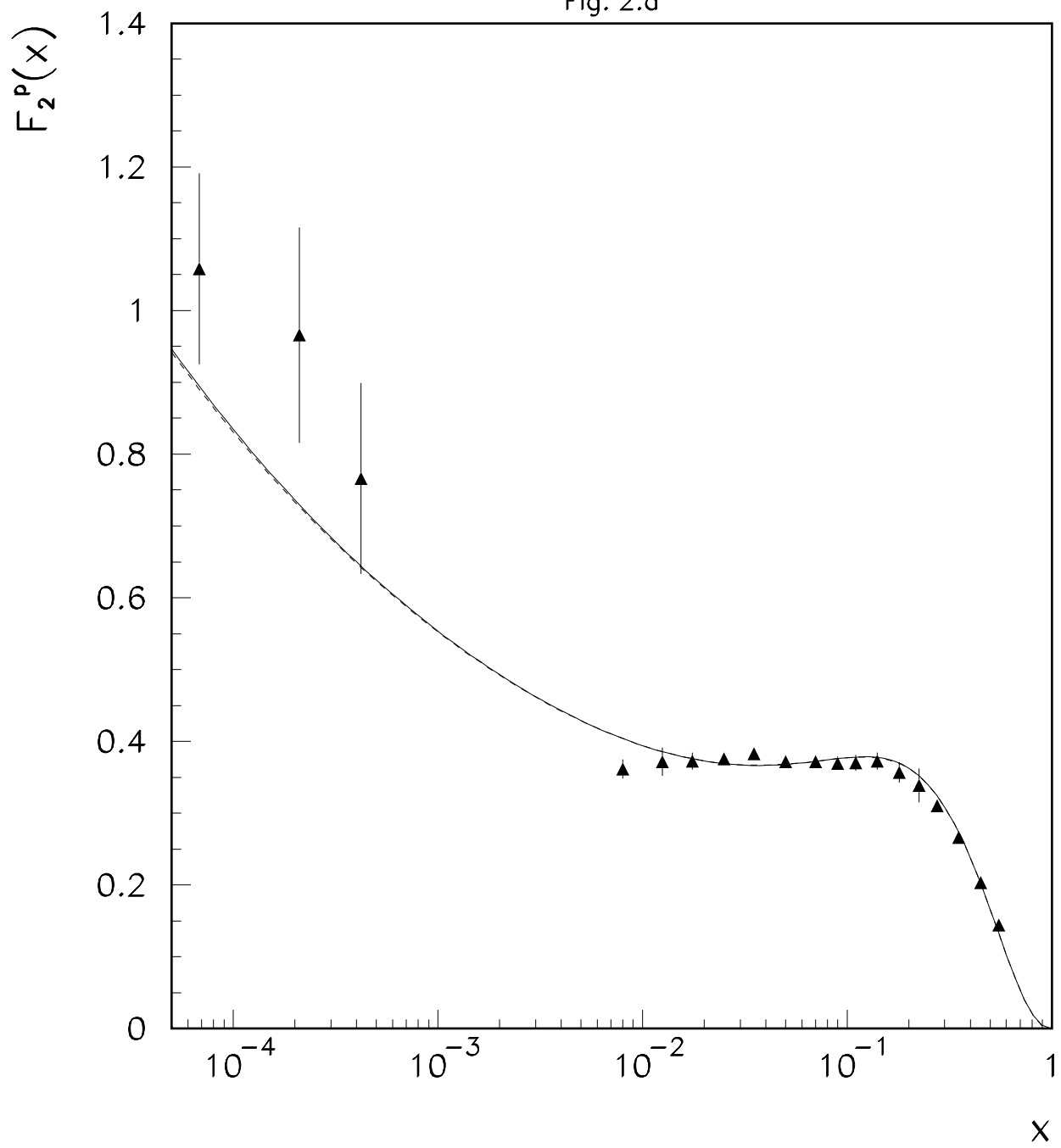


Fig. 2.b

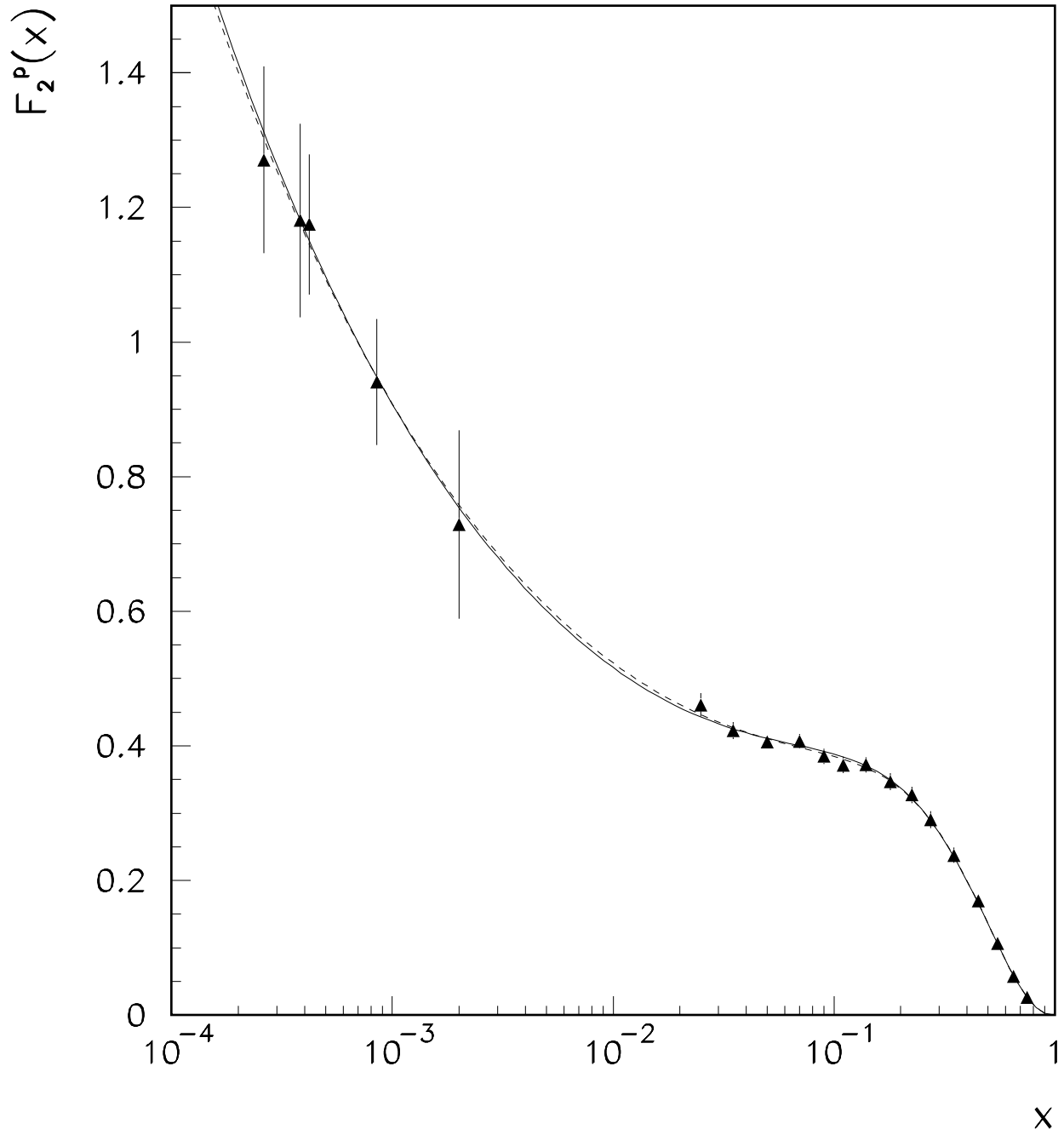


Fig. 3.a

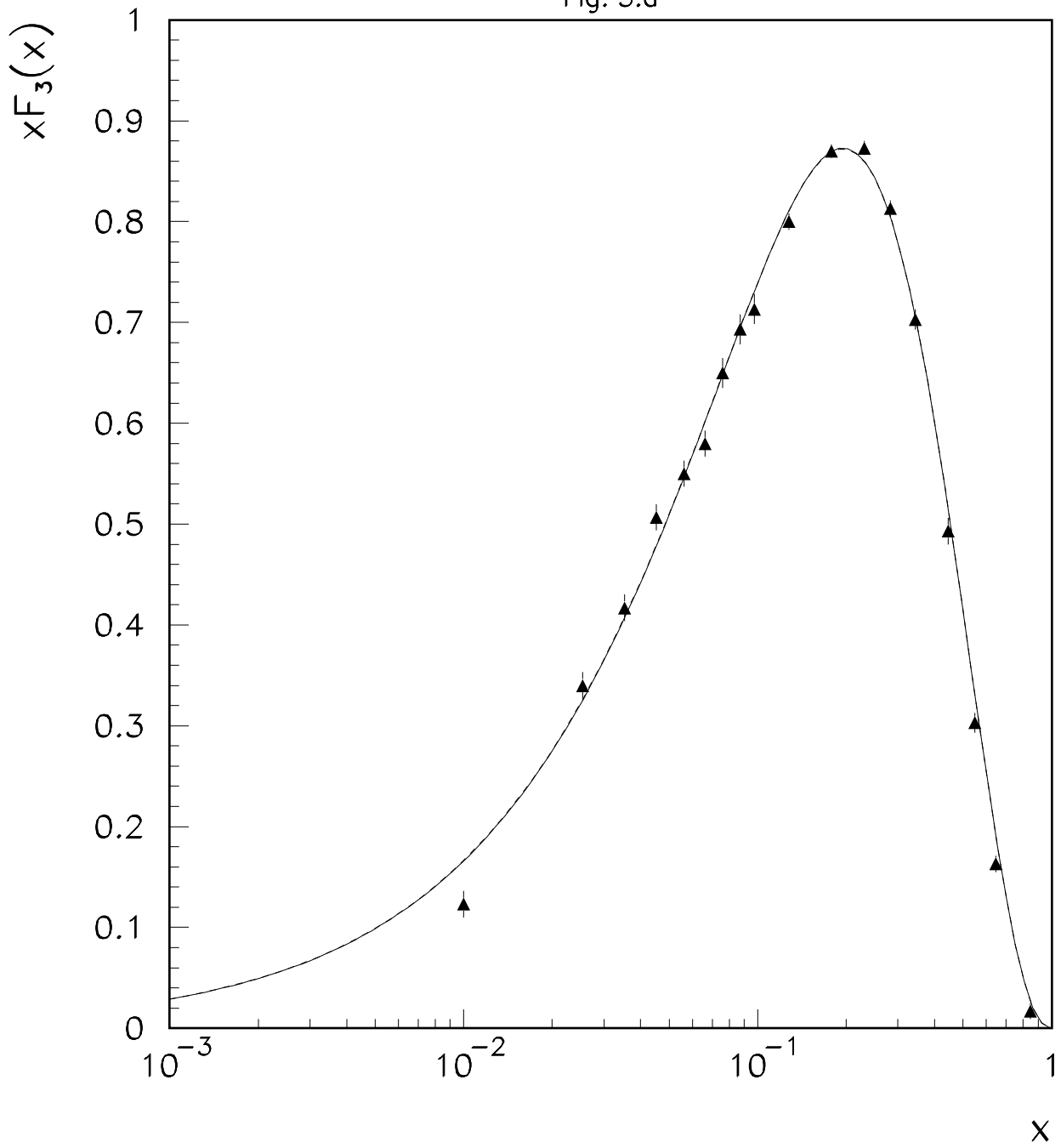


Fig. 3.b

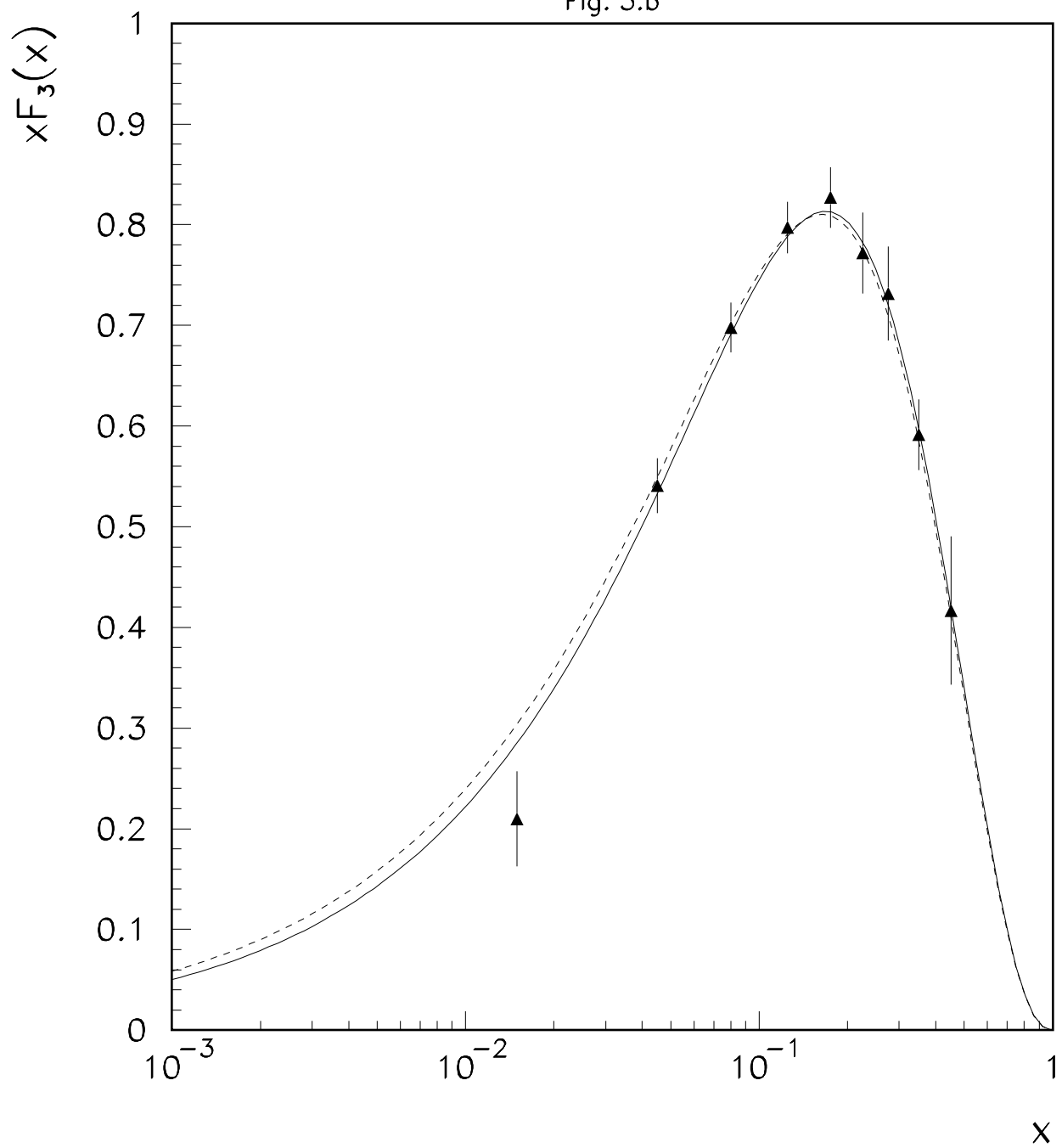


Fig. 4.a

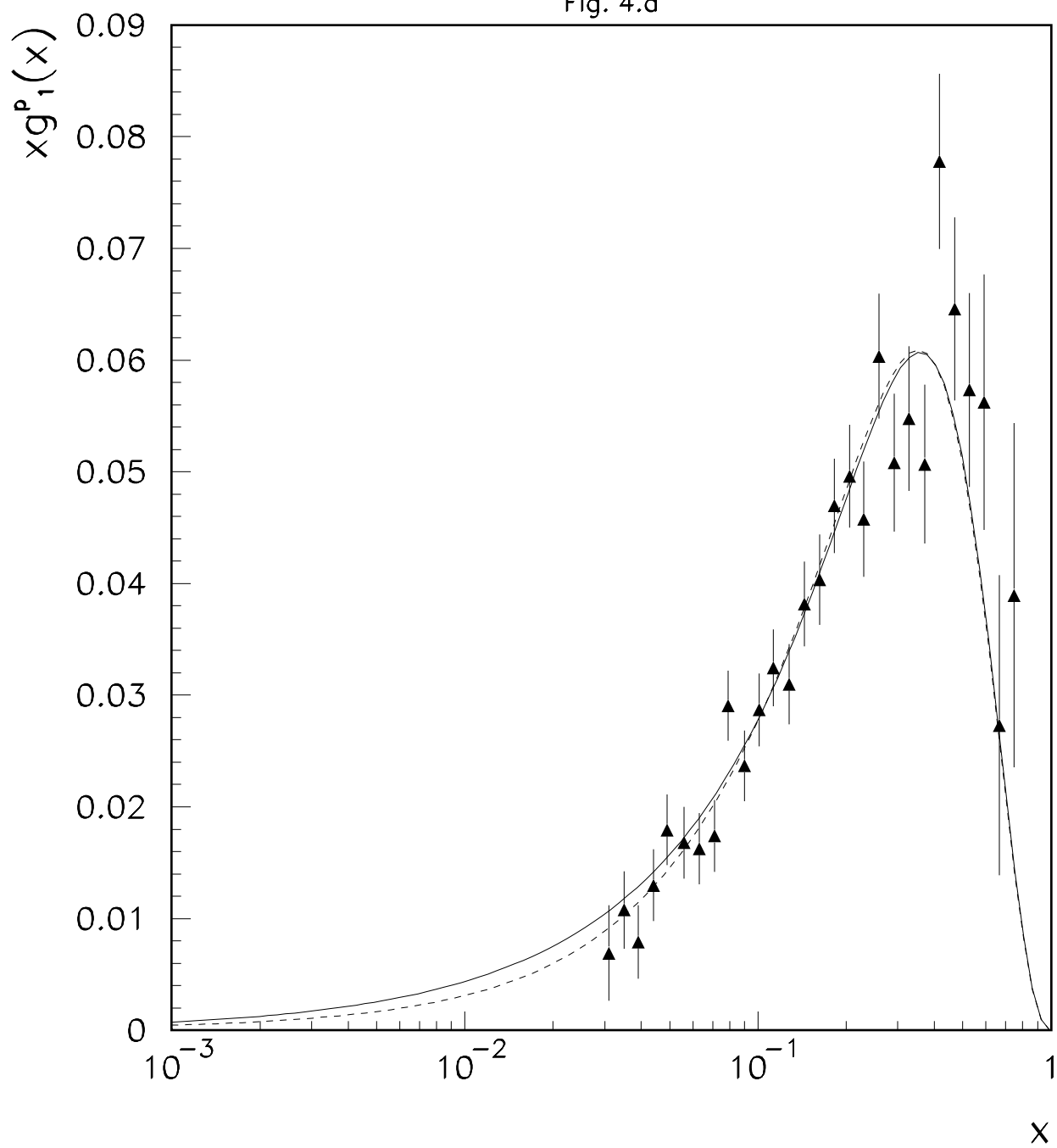


Fig. 4.b

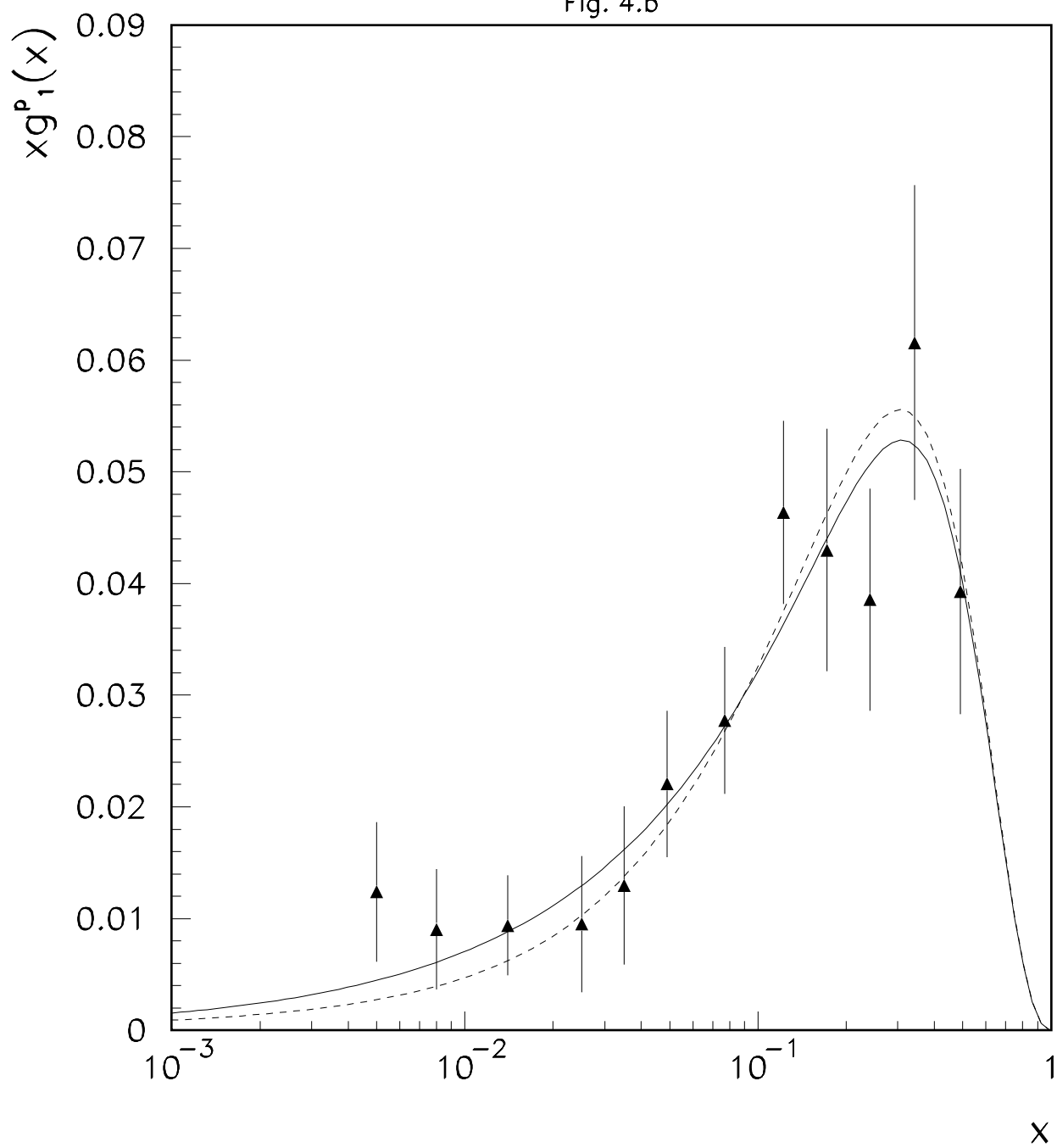


Fig. 5.a

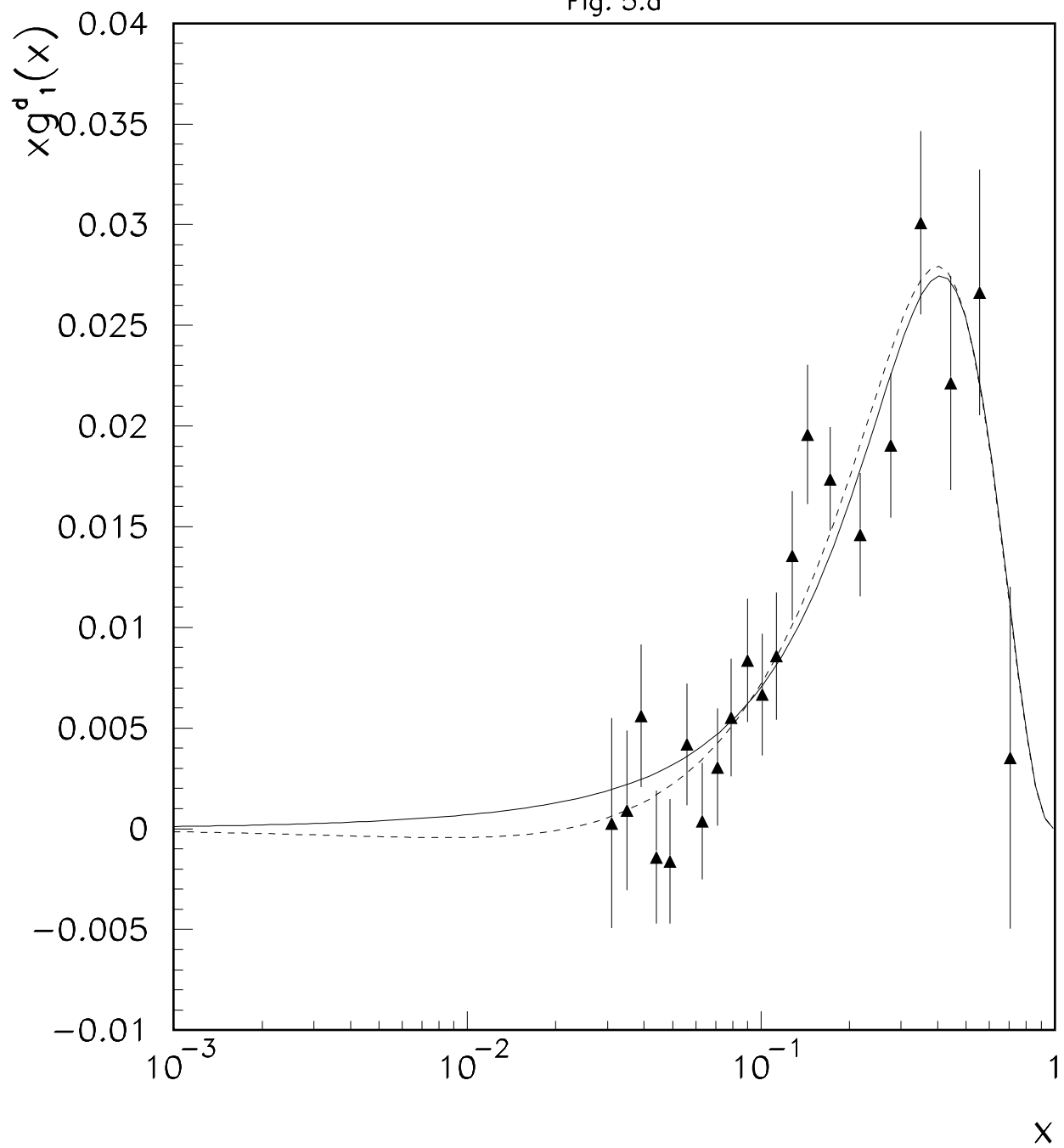


Fig. 5.b

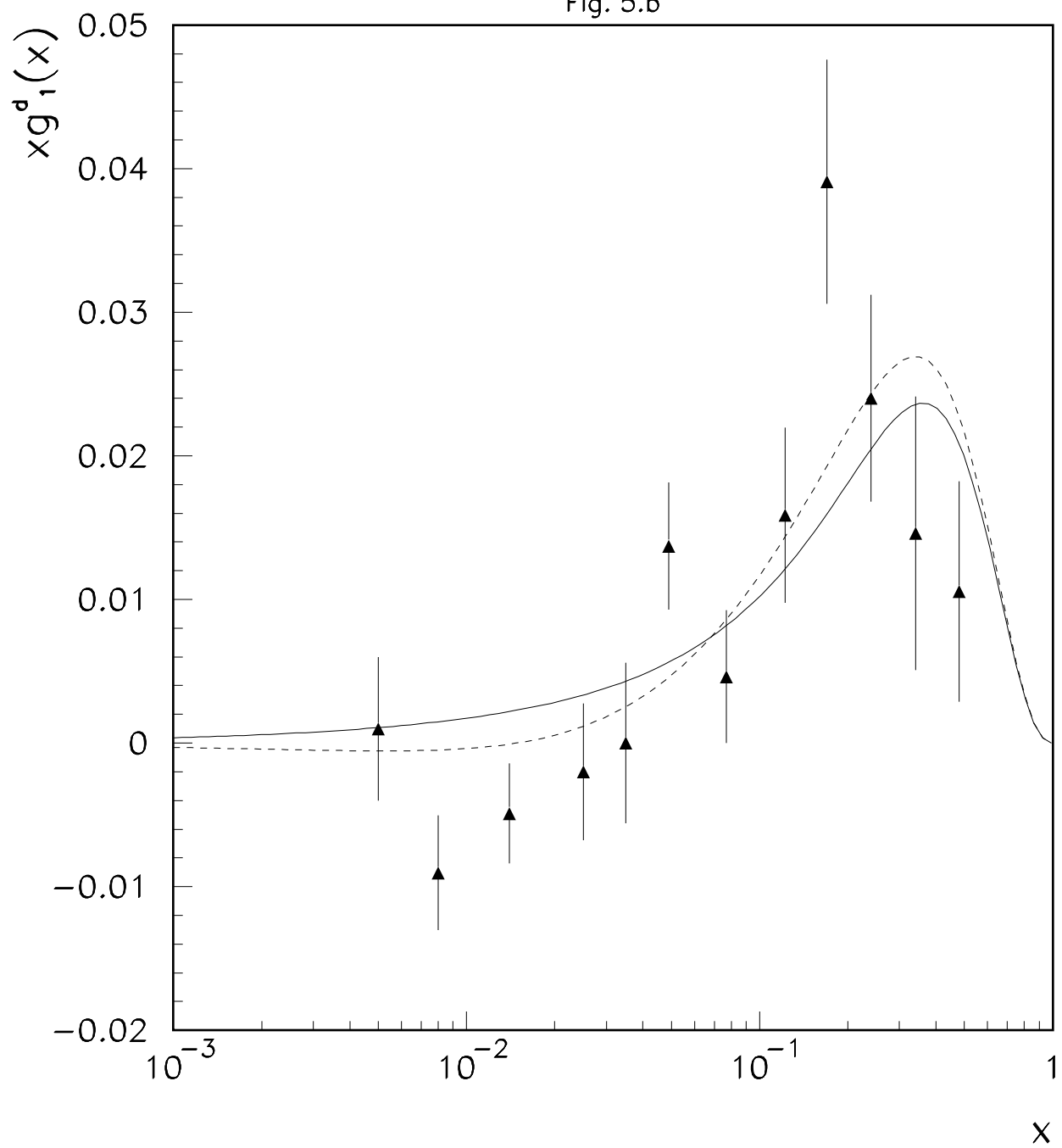


Fig. 6

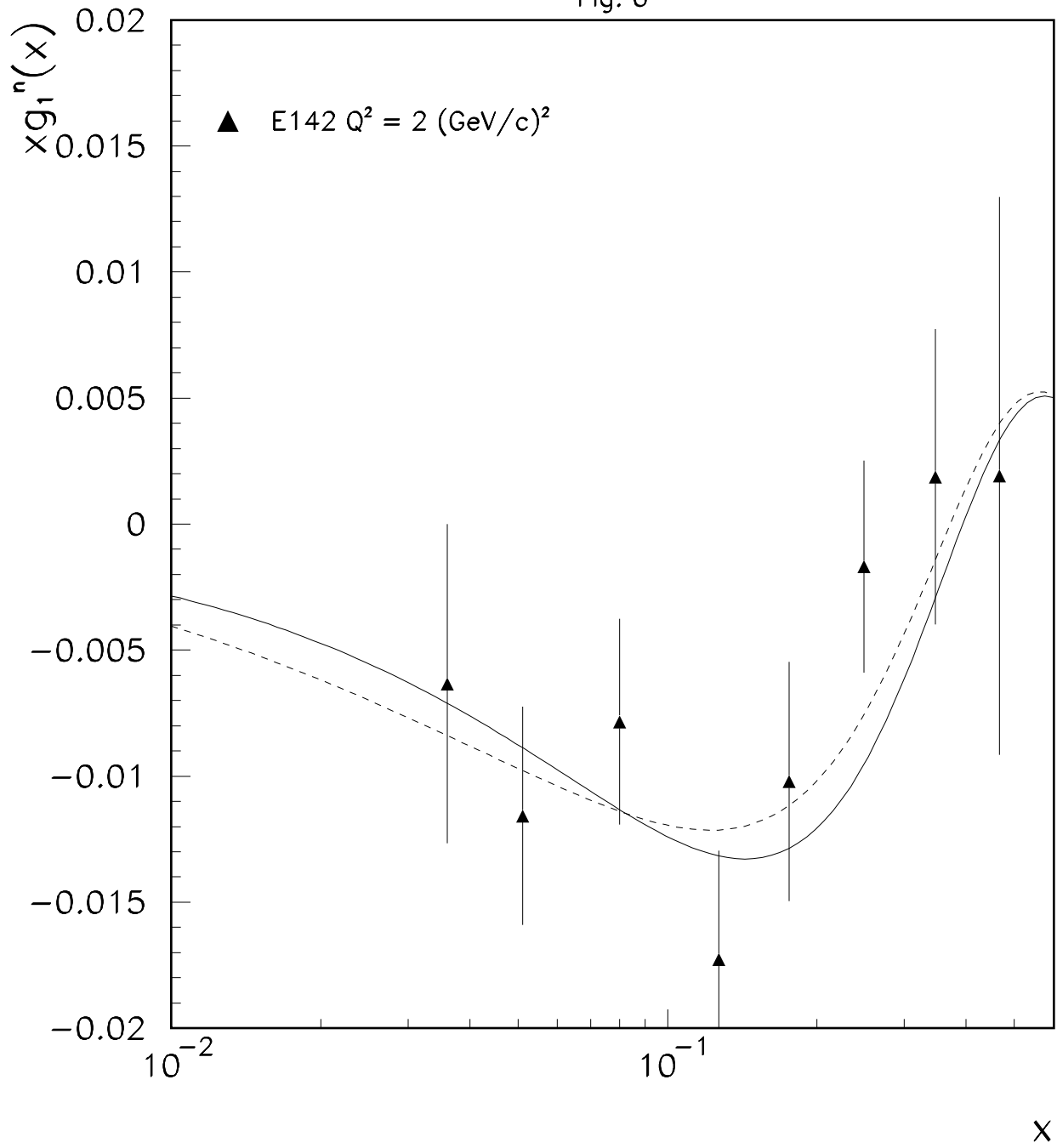


FIG. 7.a

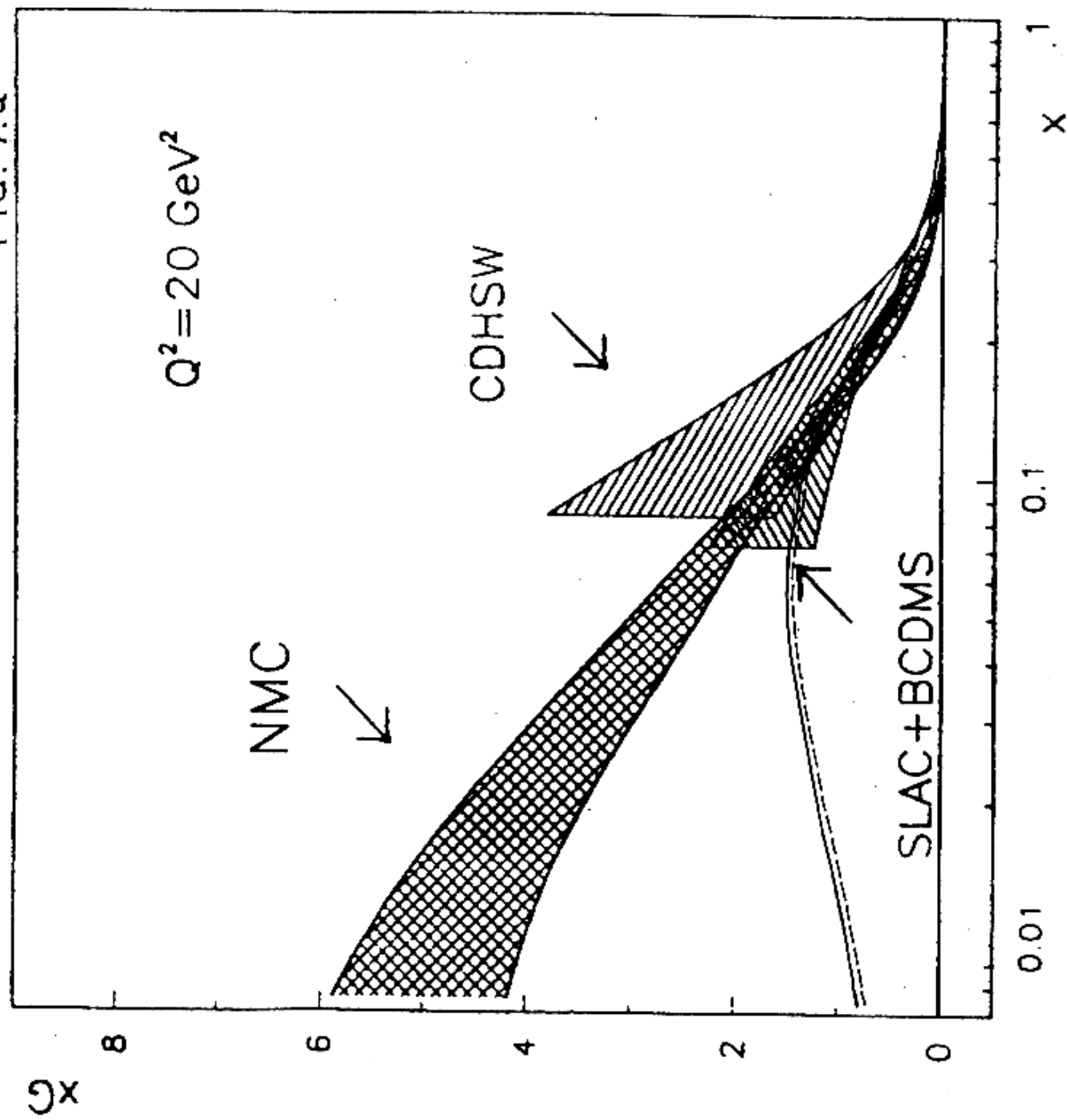


FIG. 7.b

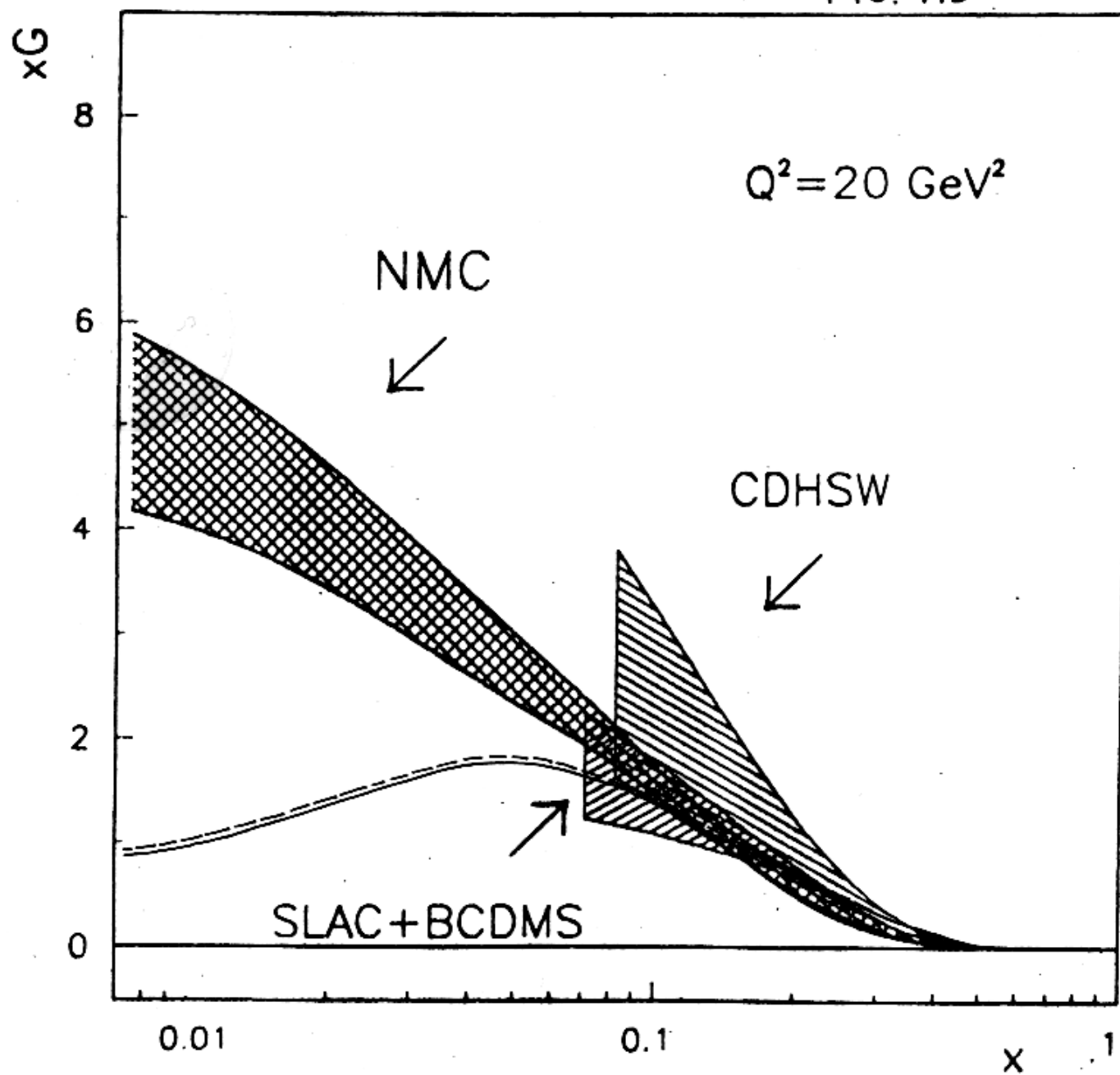


Fig. 8

